Superstructure Aerodynamics of the Type 26 Global Combat Ship

R Mateer, Dr. SA Scott, Prof. I Owen*, Dr. MD White

School of Engineering, University of Liverpool, UK
* Corresponding author. Email:i.owen@liv.ac.uk

Synopsis

The Type 26 City class Global Combat Ship is the latest design of UK frigate. Construction of the first ship, HMS Glasgow, began in July 2017 and the expectation is that it will enter service in the mid-2020s as a replacement for the Royal Navy's Type 23 Duke class frigates. The main contractor for the design and construction of the ship is BAE Systems Maritime – Naval Ships.

The Type 26 superstructure is characterised by its smooth sloping surfaces that are continuous along the ship from the fore deck to the flight deck. The tumblehome design reduces the ship's radar cross-section, as does the minimisation of curved surfaces and internal corners. The Type 26 also has a bulky mast, also with flat sloping sides, while the funnel casing around the gas turbine exhaust uptake is located aft of the main mast and relatively low on the superstructure. In comparison, the earlier Type 23 has a much more fragmented superstructure with few geometric features for reduced radar reflection; it also has a more slender mast from which the anemometers are mounted, and the exhaust uptakes are higher. Overall the aerodynamics of the stealthy Type 26 frigate will be very different to the previous Type 23, and this will affect the operational envelope of the ship's helicopters.

Recognising the importance of superstructure aerodynamics to the ship design, the University of Liverpool has been working closely with colleagues from BAE to ensure that the air flow over the ship was considered as the superstructure design evolved. The paper will describe how, within the design cycle, Computational Fluid Dynamics (CFD) has been used to analyse the unsteady flow over the full-scale ship. It will show how CFD, together with helicopter flight dynamics modelling, was used to inform design options for the superstructure geometry ahead of the landing deck. CFD was also used to inform options for locating the ship's anemometers and has been used to predict the dispersion of the ship's engine exhaust gases and the air temperature distribution in the vicinity of the flight deck.

Keywords: Ship aerodynamics; Computational Fluid Dynamics; Maritime helicopters; Ship Helicopter Operating Limits; Airwake

1. Introduction

Modern warships routinely operate with maritime helicopters. The flying environment is a challenging one: limited deck space, close proximity of superstructure, deck motion, possible visual degradation due to spray and rain, and the unsteady air flow in the vicinity of the flight deck. The unsteady air flow, or ship airwake as it is known, is due to the combination of the ship's forward speed and the prevailing wind and is often cited by pilots as being the most challenging factor when recovering to a ship in strong winds (Lumsden and Padfield, 1998). The safe operational envelope for a particular helicopter/ship combination is defined by the Ship-Helicopter Operational Limits, or SHOL, which is specified in terms of maximum allowable wind speed for different wind directions. A typical SHOL envelope is shown in Figure 1 where it can be seen, for example, that it is deemed safe to land the helicopter for wind speeds from ahead of up to 50 knots, while for winds coming from a relative direction of 45° off the starboard (Green 45) the maximum wind speed is 30 knots.

Authors' Biographies

Rebecca Mateer is a PhD candidate in naval aerodynamics at the University of Liverpool, having previously obtained her BEng degree in Aerospace Engineering with Pilot Studies at the University of Liverpool.

Dr Sarah Scott obtained her PhD in naval aerodynamics from the University of Liverpool in 2018, having previously obtained a BEng degree in Aerospace Engineering from the University of Liverpool.

Prof Ieuan Owen is Emeritus Professor of Mechanical Engineering in the School of Engineering at the University of Liverpool where he leads the research into ship superstructure aerodynamics.

Dr Mark White is a Senior Lecturer and lead academic for flight simulation activities the School of Engineering at the University of Liverpool, where he leads all of the flight simulation and simulation fidelity research including ship-air integration.

 http://doi.org/10.24868/issn.2515-818X.2018.038

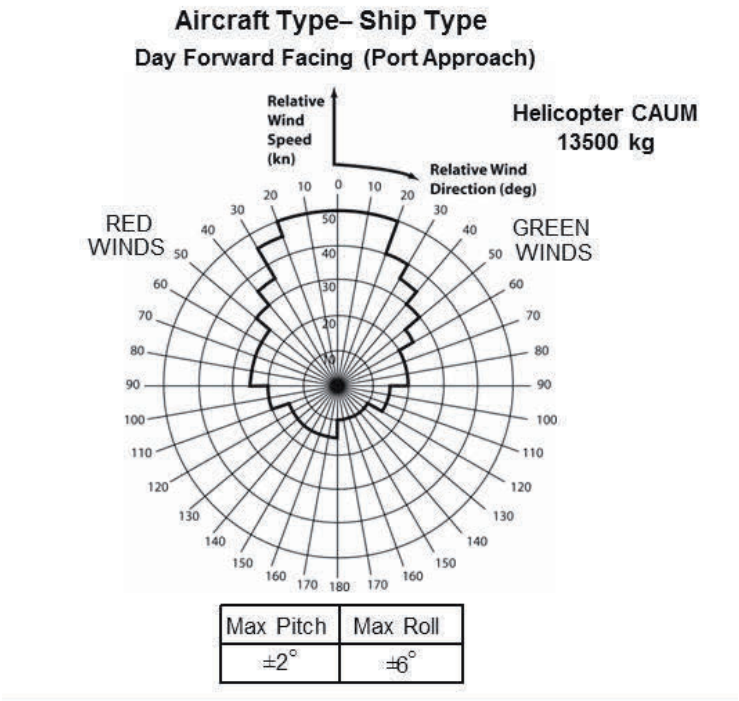

Figure 1: Representation of typical SHOL diagram

The design of a modern helicopter-enabled warship takes into account the flight deck, hangar, and other aviation services; however, consideration of the ship superstructure aerodynamics is not so prominent. Traditionally, once the ship design has been fixed, wind tunnel models have been made and used to examine the air flow over the ship, possibly including an assessment of exhaust gas dispersion and flow distortion at the locations identified for placement of the ship's anemometers. However, the effect of the ship's aerodynamics on the helicopter will not be known until the ship is built and undergoes at-sea flight trials.

In recent years there has been significant research into the use of Computational Fluid Dynamics (CFD) to model the unsteady air flow over naval ships, and into the use of mathematical flight dynamics models of a helicopter to assess how that air flow will affect the aircraft and pilot workload. These technological advances have enabled helicopter launch and recovery operations to be simulated in motion-base flight simulators where piloted deck landings have been conducted to create simulated SHOLs (Roscoe and Wilkinson, 2002; Turner et al., 2006; Hodge et al., 2012).

The latest generation of frigate that is due to enter service with the Royal Navy in the mid-2020s is the Type 26 City class Global Combat Ship, which will replace the Type 23 Duke class. The Type 26 will operate with Merlin and Wildcat maritime helicopters. Images of the two ships are shown in Figure 2. As can be seen, there are significant differences in the superstructures of the two ships, notably the clean lines of the newer Type 26, its sloping sides and much reduced equipment and systems on the superstructure. The Type 26 also has a bulky enclosed main mast, aft of which is the funnel from which the gas turbine exhaust gases are discharged. Much of the design characteristics are driven by the requirements for reduced Radar Cross Section (RCS), but the geometry of the superstructure will also affect its aerodynamics and therefore the operational envelope of the ship's helicopter. A similar design evolution can be seen between the Daring class Type 45 destroyer currently in service with the Royal Navy, and its predecessor the Sheffield class Type 42.

During the design phase of the Type 26, the opportunity has been taken to apply the modelling and simulation techniques referred to above to the evolving design of the ship superstructure. This paper will illustrate how CFD has been used to predict the air flow over the ship, and how this affects the dispersion of the exhaust gases from the gas turbine and the flow distortion at the anemometer positions, all of which have a bearing upon helicopter operations. The paper will also describe how a mathematical model of a helicopter's flight dynamics has been integrated with the CFD-generated ship airwake to assess how changes to the superstructure geometry ahead of the flight deck are expected to impact on a helicopter. Comparisons will also be made between the aerodynamics of the Type 26 and its predecessor, the Type 23. The work was undertaken by the University of Liverpool on behalf of, and in collaboration with, BAE Systems Maritime – Naval Ships.

 http://doi.org/10.24868/issn.2515-818X.2018.038

Figure 2: Type 26 City Class Global Combat Ship (top) and Type 23 Duke Class Frigate (bottom)

2. The Ship Airwake

As described above, the ship airwake is the disturbed air which flows over the ship due to a combination of its forward motion and the prevailing wind. When using CFD to create ship airwakes for use in flight simulation it is important to use what are known as time-accurate or Scale-Resolving Simulation (SRS) methods which compute the three dimensional velocity components throughout the computational domain at different time steps. The unsteady flow field can then be used to impose unsteady aerodynamic loads onto the aircraft model; it can also be used to provide a record of unsteady velocities at the anemometer positions and can illustrate the time-varying air temperatures due to the ship's engine exhaust gases. In the CFD simulations being described in this paper, the SRS methodology was Detached Eddy Simulation, and the flow field was calculated at 100 Hz, i.e. every 0.01 seconds. The Type 26 is 150m long with a beam of 20m, while the Type 23 is 130m long with a beam of 16m. The CFD computations and resulting data files are therefore very large and require the use of high performance computers. A detailed description of the CFD methodology is beyond the scope of this paper, but is given by Forrest and Owen (2010).

The first requirement for the CFD is an accurate three-dimensional digital drawing of the ship. Figure 3 shows one of the Type 26 geometries that was used in the study and which was produced from general arrangement CAD data provided by BAE. While it is important that the geometry is an accurate representation of the ship, surface features that are typically less than 0.3m in size have little effect on the air flow but have a significant effect on the computational effort, and are therefore removed.

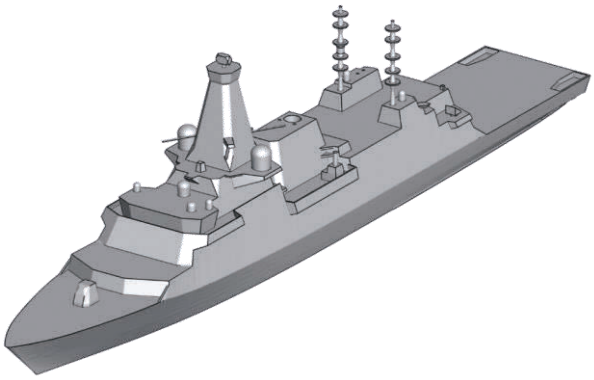

Figure 3: Typical Type 26 geometry used for calculation of CFD airwake

 http://doi.org/10.24868/issn.2515-818X.2018.038

As described by Forrest and Owen (2010), to create the unsteady airwakes it is first necessary to compute a steady state solution, before initiating the unsteady solution with a time step of 0.01 seconds. The flow approaching the ship is profiled to represent an oceanic boundary layer as this is known to influence the ship airwake. The CFD solution requires a period of time to settle to a repeatable unsteady solution; this period was typically 15 seconds (of airwake), and allows periodic flow features to develop. A fully-developed unsteady solution was then run to produce a further 30 seconds of unsteady airwake data, while the previous 15 seconds of data was discarded. The overall solution time for a single airwake was typically about 3 days using 128 processors.

Figure 4 shows the time-averaged air flow over the two ships, where the airwake is presented as Q-criterion isosurfaces which illustrate the vortical structures being shed from the edges of the superstructure, and protruding features such as the masts. Q-Criterion is a widely used parameter in CFD studies to identify and visualise vortices (Haller, 2005). The airwakes are for a Green 30 Wind Over Deck (WOD, i.e. relative wind), which are of particular interest as it is Green winds (i.e. from starboard) that impact most upon Royal Navy helicopter pilots who approach the landing deck via a lateral traverse from off the port side of the deck. It can be seen in Figure 4 that, compared with the Type 23, the Type 26 has a larger wake being shed from its bulky mast, as well as a more complex flow being shed across the flight deck from the vertical hangar edge.

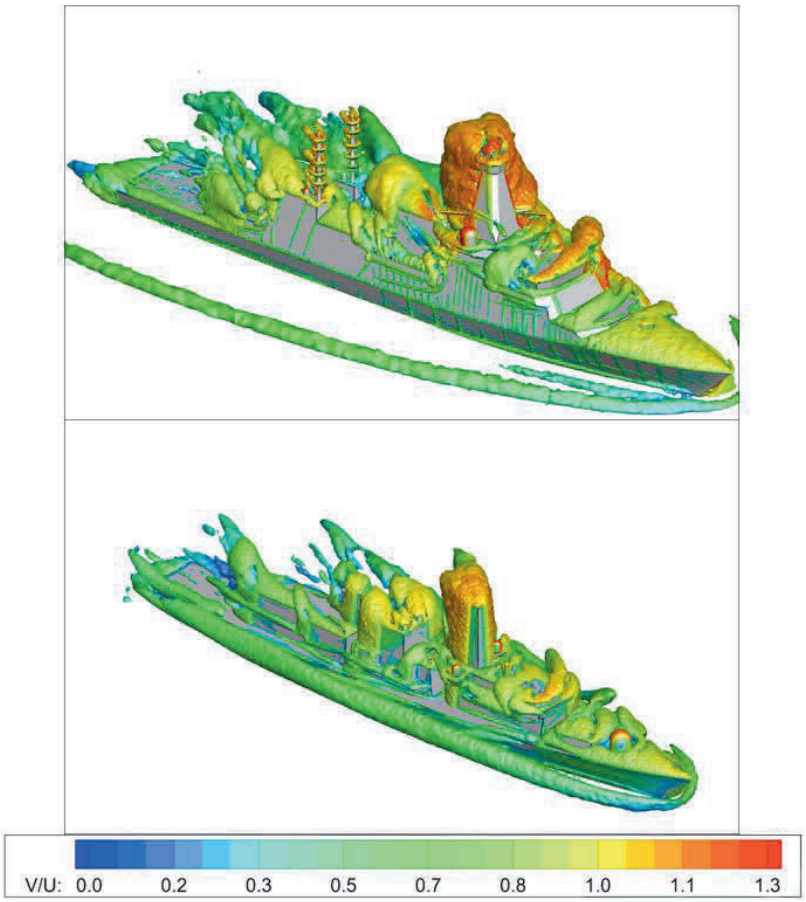

Figure 4: Airwakes for Type 26 (top) and Type 23 (bottom) in Green 30 WOD illustrated by mean isosurfaces of Q Criterion coloured by normalised velocity magnitude

It can also be seen in Figure 4 that the flow along the side of the superstructure of the Type 23 is ‘broken up’ by the irregular geometry, compared with the smooth-sided Type 26 where the air flows unimpeded along the leeward side of the ship until it separates from the vertical hangar edge to form a strong shear layer across the landing deck. How the flow across the landing decks of the two ships compare can be seen in Figures 5 and 6, where the two ships are scaled to be in proportion. Figure 5 shows mean velocity contours, normalised by free stream velocity at anemometer height in a Green 30 WOD. Looking first at the air velocities on the starboard side of the Type 23, the colour scale shows that the flow along the windward side of the superstructure just ahead of the landing deck is about 65-70% of the freestream value, while on the smoother side of the Type 26 just ahead of the landing deck it is about 80%. The regions of slower moving recirculating flow in the lee of the hangar and

 http://doi.org/10.24868/issn.2515-818X.2018.038

over the ships' decks, coloured blue, show that the recirculating flow zone is much larger for the Type 26, and the velocity gradient across the flight deck is steeper. The air flow over the deck of the Type 26 can therefore be expected to impart greater unsteady forces and moments onto the aircraft and will lead to higher pilot workload.

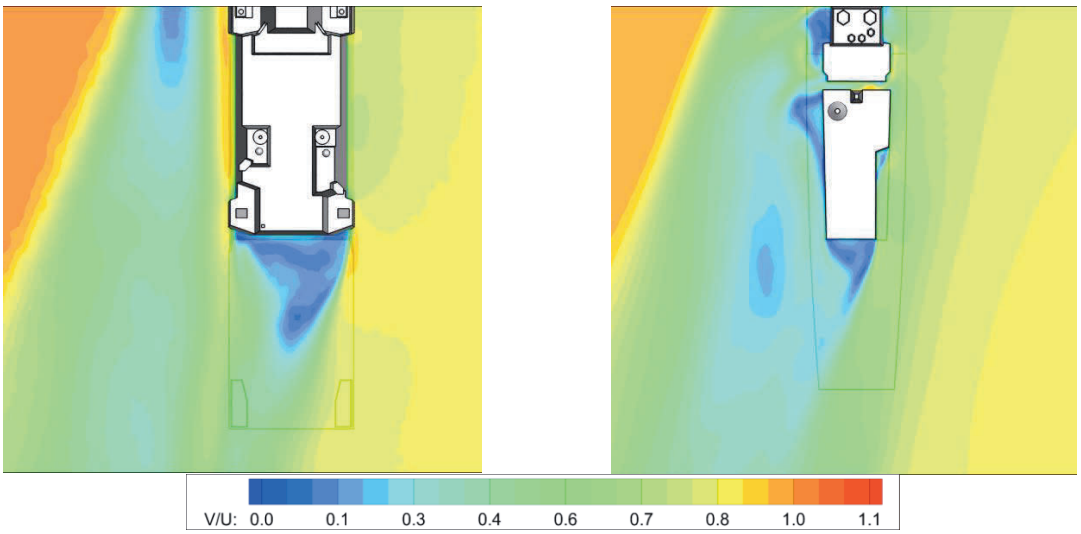

Figure 5: Airwake illustrated by contours of normalised mean velocities in horizontal plane 4m above deck height of Type 26 (left) and Type 23 (right) in Green 30 wind over deck

This observation is supported by Figure 6 which shows a cross-section of the airwake in a vertical plane across the landing decks and through the landing spot of each ship. In this case the airwake is illustrated by contours of turbulence intensity and it can be seen that the air flow over the landing deck of the Type 26 is much more turbulent than that of the Type 23 and will have a greater impact on the helicopter and the pilot workload. There are two reasons for this: one is the higher speed air flow along the smoother superstructure of the Type 26, as discussed above, and the other is that the Type 26 is a larger ship and will therefore shed larger vortices.

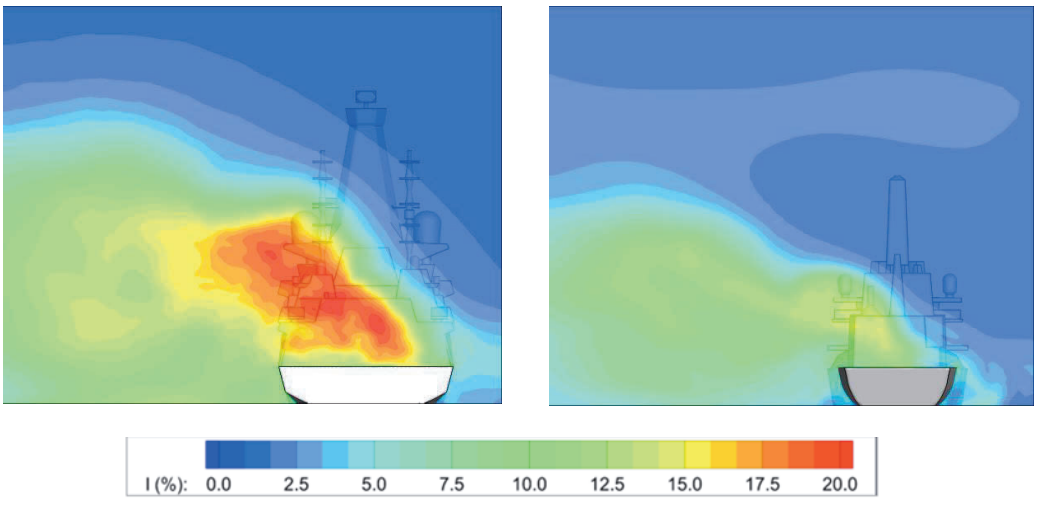

Figure 6: Airwake illustrated by contours of turbulence intensity across the landing spots for Type 26 (left) and Type 23 (right) in Green 30 wind over deck

3. Assessing the impact of superstructure geometry on a helicopter

Figures 4 to 6 above illustrate how CFD can be used to calculate the unsteady airwake around a ship. During the design of the Type 26 there were a number of design options for the superstructure geometry and an assessment was required as to how the design changes would affect the helicopter. Figure 7 shows two such design options; close scrutiny will reveal differences in the sponsons supporting the gun platforms either side of the hangar face, as well as differences in the port and starboard equipment housings, and some other smaller features. While these

 http://doi.org/10.24868/issn.2515-818X.2018.038

geometric changes can be expected to affect the air flow over the landing deck, it is more important to quantify how the changes might affect the aerodynamic loads on a helicopter. The University of Liverpool has developed a simulation assessment tool which integrates the unsteady CFD airwake with a flight dynamics model of a generic helicopter. A full description of the technique is beyond the scope of this paper but has been described by Kaaria et al. (2013). In brief, the three dimensional unsteady velocity components in the airwake are applied to the surfaces of a helicopter mathematical flight model, particularly the main rotor blades, the tail rotor and the fuselage. By holding the helicopter model stationary while it is immersed in the airwake over the deck it is possible to record the unsteady forces and moments that are being imposed onto the aircraft for the 30 second duration of the airwake. The mean value of the loads in each axis give an indication of how much control the pilot will need to apply, while the standard deviation, or root-mean-square, of the unsteady loads in each axis will give an indication of how much control activity the pilot will need to apply, and hence how much workload.

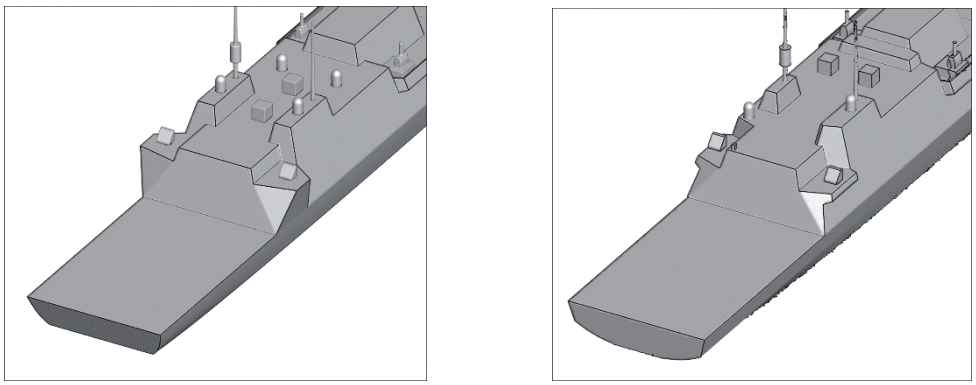

Figure 7: Two early design evolutions of the Type 26 Global Combat Ship, version A (left), version B (right)

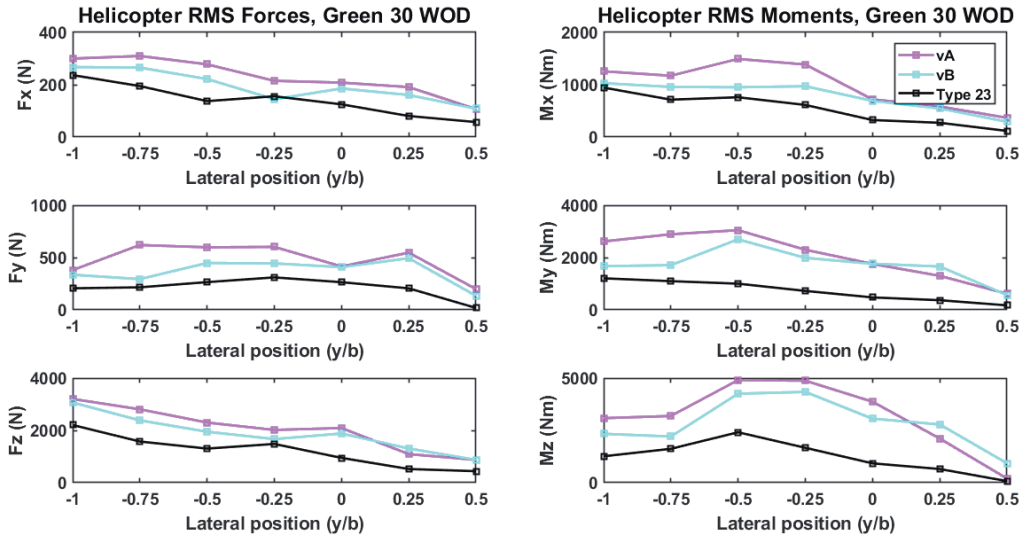

Figure 8: Unsteady aerodynamic forces and moments on helicopter flight model in a Green 30 airwake

Figure 8 shows the root mean square values (RMS) of the unsteady forces applied to the helicopter in the longitudinal axis, Fx, lateral, Fy, and vertical, Fz, as well as the roll moment, Mx, pitch moment, My, and yaw moment, Mz. The RMS loads are plotted for seven different positions of the stationary helicopter along a lateral line cross the flight deck, passing through the landing spot. The position y/b=0 corresponds to the landing spot, while ±0.5y/b correspond to the port and starboard deck edges (b is the width of the flight deck). In this case the WOD is Green 30. While it is difficult to fully appreciate what the data is showing in such a short discussion, the pink line corresponds to the RMS loads for the version A geometry above, and the blue line corresponds to version B. The higher values in all axes and most positions shows that the version A geometry produces an airwake over the deck that will be more demanding for the helicopter and pilot. One reason for the increased unsteady loads

 http://doi.org/10.24868/issn.2515-818X.2018.038

for version A is that the sloping sponson supporting the starboard gun platform deflects the oncoming wind that flows along the starboard side of the ship upwards above the height of the hangar and across the flight deck just above the helicopter's main rotor; the unsteady flow will therefore be drawn into the rotor and will create unsteady pitch and roll moments and unsteady lift forces. As a result of the analysis, the sloping sponson option was therefore rejected early in the design process. Also shown in Figure 8, for comparison, are the unsteady loads on a helicopter in the airwake of a Type 23 frigate. It can be seen that the unsteady loads are lower for this ship, and that is mainly due to the airwake characteristics shown earlier in Figures 5 and 6.

4. Assessment of air flow at anemometer positions

As well as impacting directly onto the helicopter, the disturbed flow of the ship's airwake also affects the accuracy of the ship's anemometers. As shown earlier in Figure 1, the safe operational envelope for the helicopter is defined by the SHOL. The boundaries of the SHOL are determined by at-sea flight trials where test pilots fly repeated deck landings at different wind angles and wind speeds to find the limiting conditions at which it is safe for a fleet pilot to launch and recover the helicopter. While the wind speed and direction during the trials are usually measured by dedicated temporary anemometers mounted on tall masts at the bow of the ship, in an attempt to avoid the ship's airwake, the readings have to be correlated with the ship's own anemometers, and for every sortie afterwards it will be the ship's anemometers that measure the wind speed and direction. If the ship's anemometers are incorrect or unreliable, then the SHOL will not be correctly specified in the first instance, and neither will the wind condition be reliably measured for every sortie conducted thereafter. Accurate readings from the ship's anemometers are therefore essential for a reliable SHOL.

The operational parameters for the anemometers are prescribed by Defence Standard 00-133 (2015), extracts from which are shown below:

Anemometers should be:

- positioned in clear air above the edge of the boundary layer created by the ship's superstructure
- located as high as possible on separate port and starboard yard arms
- in a space uncluttered by adjacent equipment, facing forward with at least 3.0m radius free air space around each anemometer

Accuracy of Indicators should be as follows:

- Wind Speed ± 5% error
- Wind Direction ± 5 degrees error

As was seen earlier in Figure 4, finding a location on the ship that is outside of the airwake is difficult, and the trend towards bulky enclosed masts will significantly distort the flow at the traditional anemometer locations on the main mast. Figure 9 shows head-on views of the Type 23 and Type 26 ships, with their anemometer locations identified by red squares. The perspective views of the two ships are different and in practice the two sets of anemometers are approximately the same height above sea level. The Type 23 anemometers can be expected to be in less distorted air flow because of the more slender mast and longer forward-facing yardarms on which they are mounted. The larger mast of the Type 26, however, as well as the bigger deck house and the additional equipment ahead of and in the vicinity of the anemometers, can be expected to have a greater influence on the air flow. A more detailed discussion of the aerodynamics of a bulky ship mast has been given by Mateer et al. (2016).

Figure 9: Head-on view of Type 26 (left) and Type 23 (right) showing positions of main anemometers

 http://doi.org/10.24868/issn.2515-818X.2018.038

How much the airflow at the anemometer positions will be distorted, and the identification of alternative locations, can be extracted from the CFD-generated airwakes. Figure 10 shows the air flow at the anemometer positions, indicated by small circles, for the Type 23 and Type 26 ships, for winds from ahead and 30° from starboard. The contours show the magnitude of air velocity (sum of all three components) normalised by the free stream value at anemometer height. The bigger wake in the lee of the bulkier Type 26 mast, and its influence on the flow ahead of the mast, can be clearly seen.

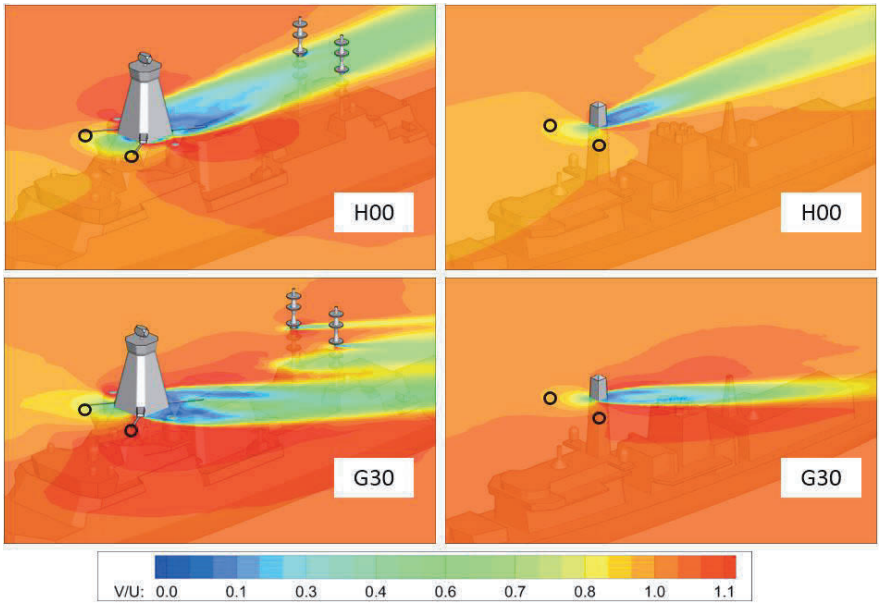

Figure 10: Air flow at anemometer positions illustrated by contours of normalised mean velocities for headwind and Green 30, for Type 26 (left) and Type 23 (right). Anemometer positions indicated by circles.

Significant detail can be extracted from the CFD, including time varying velocity components at the anemometer position, so that the variation of magnitude and direction of local air velocities can be evaluated. Figure 11 shows a plan view of the mean flow field ahead of the main mast in the plane of the anemometers for a headwind; the anemometer positions are identified by the white circles. The contours show velocity magnitude normalised by freestream velocity, while the vectors represent the velocity direction and magnitude in the horizontal plane. The clustering of the vectors around the features on the mast is due to the more dense CFD mesh in those regions. Even in the headwind, it can be seen that the differences between the freestream and the air flow at the anemometer positions are 10% in magnitude and 10° in heading. These predicted differences will inform the anemometer calibration that takes place during the ship's Air Flow Air Pattern sea trials. The CFD analysis also makes it possible to explore other candidate locations for the anemometers.

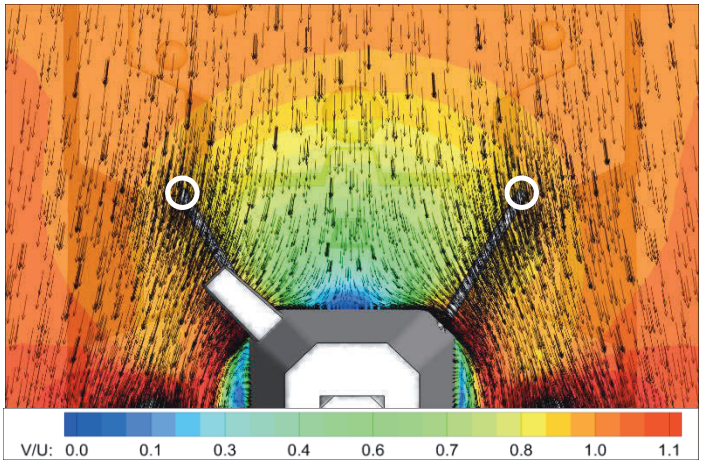

Figure 11: Local mean flow field in proximity of Type 26 anemometers.

 http://doi.org/10.24868/issn.2515-818X.2018.038

5. Assessment of ship engine exhaust dispersion.

The Type 26 will have a combined Diesel-electric and gas propulsion system (CODLAG) incorporating a Rolls Royce MT30 gas turbine with a maximum power output of 40MW. The Type 23 also operates with a CODLAG system, but incorporating two 19.5MW Rolls Royce Marine Spey engines. Both ships also operate with four Diesel generators. The volume of hot gases being exhausted, particularly from the gas turbine, can therefore be very high. The hot gases will mix with the ship's airwake and be cooled; nevertheless, there will be elevated air temperatures in areas around the flight deck and this can affect the helicopter performance. While there are no regulations or recommendations for air temperature increases over the landing decks of naval ship's due to exhaust gas efflux, there are for the offshore oil and gas industry, which is highly regulated for Health and Safety; the sources of the air temperature rises are gas turbines and flarestacks. Guidance on operating standards for helicopter landing areas on offshore platforms using helicopters registered in the UK is given by the Civil Aviation Authority in CAP437 (2016). In this document, caution is advised when the air temperatures above the flight deck rise more than 2°C above ambient, averaged over a 3 second period. There are two issues for the helicopter arising from elevated air temperatures, the first is loss of lift due to lower density air passing through the main rotor, and the second is a potential reduction in power when the heated air is drawn into the helicopter's engine. A more detailed discussion on this topic is given by Scott et al. (2015).

During the aerodynamic assessment of the Type 26, CFD analyses of the dispersion of engine exhaust gases were therefore also conducted, for numerous engine power outputs and WOD conditions. The airwake CFD analysis was modified to include the injection of hot gases into the flow domain. The gas turbine exhaust discharges from a 2.8m diameter uptake housed in a funnel casing immediately aft of the main mast, while the aft Diesel generators' two 0.5m diameter uptakes are integrated into the starboard aft equipment housing on the hangar roof just ahead of the flight deck. Figure 12 shows a cross section of the exhaust plume as it passes through a vertical plane across the Type 26 flight deck, through the landing spot, for both a headwind and a Green 30 WOD. The plume is illustrated by contours of mean temperature in degrees Celsius above ambient. The parameters of the exhaust conditions for this particular analysis were a gas turbine mass flow rate of 106 kg/s and temperature of 508°C, and two aft Diesel generator mass flow rates of 5.6 kg/s and temperatures of 430°C. The wind over deck in both cases was 27 knots and the ambient air temperature was 38°C, to simulate conditions in, for example, the Arabian Gulf.

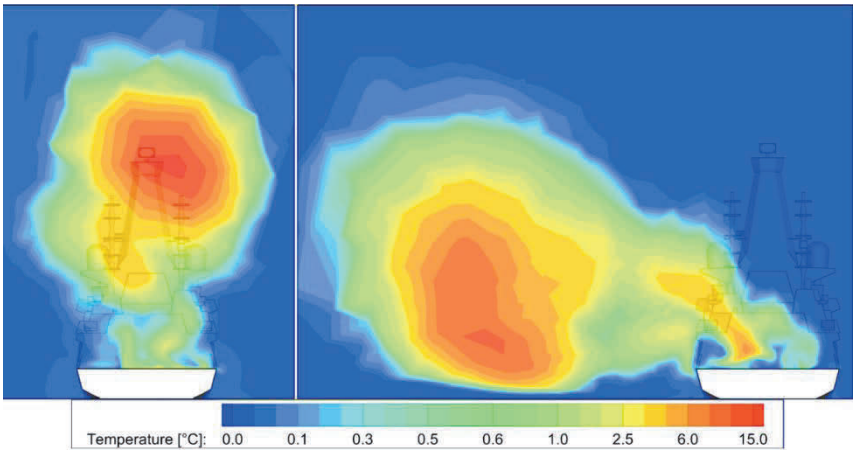

Figure 12: Contours of air mean temperatures above ambient in vertical plane through Type 26 landing spot, 27 knot Headwind and Green 30 WOD.

The temperature scale in Figure 12 is logarithmic and it can be seen that by the time the 508°C gases from the gas turbine exhaust have mixed with the airwake and are passing through the plane over the centre of the flight deck, the temperatures have significantly reduced to about 15° above ambient at the hottest part of the two plumes shown. For normal operations the pilot will translate the helicopter across the deck to the landing spot at a height where the main rotor will be just above the hangar roof. Looking at the contours in Figure 12, therefore, it can be seen that in the headwind the average air temperatures above the main rotor can be expected to be about 3°C above ambient at the centre of the deck. For the Green 30 wind the maximum average temperature is off the port side of the ship; however, the pilot will begin the landing manoeuvre by positioning the aircraft about one beam width off the port side and could therefore be drawing in air with average temperatures of about 6°C above

 http://doi.org/10.24868/issn.2515-818X.2018.038

ambient. These are not excessive temperatures, but they are higher than those considered safe by the offshore industry regulators. The air temperatures shown in Figure 12 are mean values, while in reality they will be varying with time. Fluctuating inlet air temperatures can be an issue for the helicopter engine control system and so the CFD analysis can also produce time-varying data for the air temperatures. The small area of heated air over the flight deck in the Green 30 wind is the exhaust from the Diesel generators. These are unlikely to cause a problem for the aircraft, but there might be an issue for crew comfort due to the fumes.

6. Concluding comments

Modelling and Simulation has been applied during the design process of the Type 26 Global Combat Ship to help understand how different design evolutions will affect the superstructure aerodynamics from the perspective of the ship's helicopter. The simulation methods that have been applied are those of Computational Fluid Dynamics and Flight Dynamics Modelling. The use of piloted flight simulation conducted in motion-base flight simulators has also be alluded to, but has not been part of the project reported in this paper. This project is probably the first time that the effect of the ship's design on the operational envelope of the helicopter has been considered during the design process. It would not be true to say that the modelling and simulation techniques described in this paper have led the design process, it was more a case of evaluating design changes after they had been made, mainly because of the complexity of the design and the competing priorities across the various ship systems. Nevertheless the final geometry of the gun platforms discussed in the paper was chosen based on the results of the analysis described in section 3.

A feature of modern warships is their stealth characteristics, which have been illustrated in the paper by comparing the superstructure geometries of the Type 26 and Type 23 frigates. The smoother slab-sided ships with significantly fewer topside features and equipment have a much reduced RCS, but a consequence is that the air flow over the helicopter flight deck can be significantly affected. Perhaps more important, but less obvious, is the mounting of the ship's anemometers on the large enclosed main mast, while trying to apply conventions and design rules that belong to earlier designs of ships. An accurate measurement of the speed and direction of the wind over deck is essential for establishing and maximising the SHOL envelop. The conventional methods for measuring wind speed and direction need reassessing in the light of modern warship design.

To the authors' knowledge there have been no accidents or incidents where naval helicopters have experienced problems due to ship engine exhaust, other than complaints of fumes in the cockpit. Nevertheless, there have been accidents on offshore platforms (Civil Aviation Authority, 2000), which have led to recommendations for air temperature limits over the flight deck. The analysis of the ship's engine exhaust gas dispersion presented in this paper has shown that, for the conditions tested, the air temperatures over the flight deck are just a few degrees above ambient. However there are areas in the core of the plume with higher temperatures, although these are some 20m above the main rotor during a normal helicopter recovery.

Acknowledgements

The financial support and the collaboration of colleagues at BAE Systems Maritime – Naval Ships, Scotstoun, is gratefully acknowledge, as is the ongoing support of ANSYS Inc.

References

Civil Aviation Authority, 2000. Research On Offshore Helideck Environmental Issues. CAA Paper 99004, London.

Civil Aviation Authority, 2013. CAP 437: Standards for Offshore Helicopter Landing Areas, London.

Forrest, J., Owen, I., 2010. An investigation of ship airwakes using Detached-Eddy Simulation. In: Computers and Fluids, 39(4), pp. 656-673.

Haller, G., 2005. An objective definition of a vortex. In: J. Fluid Mechanics, Vol. 525, pp. 1-26.

Hodge, S.J., Forrest, J.S., Padfield, G.D., Owen, I. 2012. Simulating the Environment at the Helicopter-Ship Dynamic Interface: Research, development and Application. In: Aeronautical J., 116 (1185), 2012, 1155-1184.

Kääriä, C.H., Forrest, J.S., Owen, I. 2013. The Virtual AirDyn: a simulation technique for evaluating the aerodynamic impact of ship superstructures on helicopter operations. In: Aeronautical J., 117 (1198), 1233-1248.

Lumsden, B., Padfield, G.D. 1998. Challenges at the Helicopter-Ship Dynamic Interface. In Proceedings Military Aerospace Technologies – Fitec '98, IMechE Conference Transactions, Institution of Mechanical Engineers, Wiley, UK.

 http://doi.org/10.24868/issn.2515-818X.2018.038

Mateer, R., Scott, P., White, M., Owen, I., 2015. The Aerodynamics of a Bulky Main Mast. In Proceedings of American Society of Naval Engineers Annual Launch and Recovery Symposium, Baltimore, USA.

Ministry of Defence, 2015. Defence Standard 00-133, Requirements and Guidance for the Aviation Arrangements in Surface Ships: Part 2 - Guidance for the Design and Construction of Aviation Requirements, UK Ministry of Defence.

Roscoe, M.F., Wilkinson, C.H. 2002. DIMSS – JSHIP's Modeling and Simulation Process for Ship Helicopter Testing and Training. In: AIAA Modeling and Simulation Technologies Conference and Exhibition, AIAA 2002-4432, , Monterey, CA.

Scott, P., White, M., Owen, I., 2015. Unsteady CFD Modelling of Ship Engine Exhausts and Over-Deck Air Temperatures and the Implications for Helicopter Operations. In: Proceedings 71st American Helicopter Society Annual Forum Virginia Beach, Virginia, USA.

Turner, G., Clark, W., Cox, I., Finlay, B., Duncan, J. 2006. Project SAIF – assessment of ship helicopter operating limits using the Merlin helicopter simulator. In: AHS 62nd Annual Forum, Phoenix, AZ, 9-11 May.

 http://doi.org/10.24868/issn.2515-818X.2018.038